ANALYSIS OF SELF-SUSTAINED INSTABILITIES ON COMPRESSIBLE LAMINAR SEPARATION BUBBLES

Elmer Mateus Gennaro, elmer.gennaro@sjbv.unesp.br[1]
Bruna Dias Pires de Souza, bdpsouza@gmail.com[1]
Daniel Rodríguez, dani@mec.uff.br[2]

[1] São Paulo State University (UNESP), Campus of São João da Boa Vista, São João da Boa Vista, SP 13874-149, Brazil
[2] Laboratory of Theoretical and Applied Mechanics (LMTA), Graduate Program in Mechanical Engineering (PGMEC), Department of Mechanical Engineering, Universidade Federal Fluminense, Niterói, RJ 24210-240, Brazil

Abstract: *Separation bubbles have been demonstrated to have an intrinsic instability mechanism, which results in the appearance of spanwise-periodic three-dimensional structures. The instability mechanism responsible for three-dimensionality was found to become active, in incompressible flow, under conditions in which wavelike, two-dimensional perturbations are only convectively unstable, and thus would require of continuous external excitation to dominate the physics. The aim of this work is to extend this analysis to compressible subsonic separation bubbles, as compressibility could alter the qualitative picture. Direct numerical simulations are carried out to obtain two-dimensional base flows, determining the conditions for the appearance of self-sustained two-dimensional oscillations. For those bubbles that remain steady in the two-dimensional simulations, a linear instability analysis based on two-dimensional eigenmodes - referred to as biglobal analysis in the literature - is applied to the study of the stationary three-dimensional instability. The effect of Reynolds and Mach numbers on both kinds of instabilities and the conditions under which they become active are also documented.*
Keywords: *separation bubbles, compressible subsonic flow*

1. INTRODUCTION

The understanding and identification of the physical instability mechanisms responsible for the appearance of unsteadiness and three-dimensionality on laminar separation bubbles can provide a fundamental insight into the aerodynamic characteristics of airfoils at stall conditions, and guide the development of strategies for the control of separated flows. Due to the combined effect of the airfoil curvature and angle of attack, an adverse pressure gradient appears past the nose suction peak. If this pressure gradient is strong enough, the laminar boundary layer will separate and give rise to a detached mixed layer, which encloses a region in which fluid motion is much slower and in the opposite direction, referred to as recirculation region. The mixing layer is very unstable to inviscid instability of the Kelvin-Helmholtz type (Lin, 1955), and eventually the laminar flow will transition to a turbulent regime. Finally, the strong mixing provided by turbulence forces the flow to reattach.

The instability and transition characteristics of laminar separation bubbles have been addressed by many experimental and numerical works considering the simple set-up of a flat-plate boundary layer subjected to an external flow deceleration, equivalent to an adverse pressure gradient (Rist and Maucher, 1994, 2002; Diwan and Ramesh, 2012; Marxen *et al.*, 2013; Embacher and Fasel, 2014). Environmental disturbances are presented naturally in wind tunnel experiments, while controlled disturbances are commonly introduced at the inlet of the computational domain, that feed on the separated-flow instability trigger the laminar-turbulent transition process. Thus, the details of the transition process depend completely on the kind of external perturbations that are imposed upstream of the separation. In fact, it has been demonstrated that many different instability mechanisms, linear and nonlinear, may play a role in the amplification of environment or externally imposed perturbations. However, this classic description of the transition process on laminar separation bubbles is based on what is called "the amplifier behavior of laminar separation bubbles" which assumes that external perturbations are present and consequently dominate the physics.

Much less work has been done considering the potential of laminar separation bubbles of presenting self-destabilizing mechanisms, that could initiate transition in scenarios in which external disturbances are very weak or even totally absent. These intrinsic or self-excited instability mechanisms acting on nominally two-dimensional and steady separation flow would be responsible for the break-down of the two main symmetries existing in the set-up, namely the invariance with respect to time and with respect to the third, spanwise direction.

Considering incompressible flow, Rodríguez *et al.* (2013) studied the competence of two self-excited instability mechanisms in order to ascertain which of the two possible mechanisms should be expected to dominate. The first mechanism corresponded to a global oscillator that turns the steady two-dimensional bubble into an unsteady one, ultimately leading to vortex shedding; the second one was a three-dimensional global eigenmode, associated to a centrifugal instability, that was conjectured by Dallmann (1988) and then confirmed by Theofilis *et al.* (2000). Rodríguez *et al.* (2013) showed the dominance of the three-dimensional instability, concluding that, in the absence of external forcing, incompressible laminar separation bubbles should be expected to become three-dimensional and give rise to spanwise periodic flow topologies as described by Rodríguez and Theofilis (2010).

The implications of this discovery were addressed by Rodríguez and Gennaro (2015); Gennaro *et al.* (2015). Provided

that unforced bubbles in a perfectly two-dimensional and time-independent set-up become three-dimensional as a result of a self-excited global flow instability, secondary instabilities could appear resulting from the steady distortion of the separation bubble that give rise to self-sustained oscillations. This possibility was confirmed in Rodríguez and Gennaro (2015) for separation bubbles characterized by a reversed flow velocity lower than that expected for the global oscillator to appear as a primary instability, explaining the process through which an unforced bubble becomes unsteady and three-dimensional and initiates the laminar-turbulent transition.

The aim of this work is to extend the previous analyses to compressible subsonic separation bubbles, and to investigate if the compressibility could alter the qualitative picture. A flat-plate boundary layer subjected to an adverse pressure gradient was considered again as the model configuration for laminar separation bubble. The bubble considered here is of the kind that occurs in the leading edge of a thin airfoil when it is at high angle of attack. For this, direct numerical simulations were carried out to obtain two-dimensional base flows.

2. METHODOLOGY

The transition process from laminar to turbulent flow is generally associated to instabilities with the reference laminar flow, named base flow. Small perturbations grow in amplitude extracting energy from mean flow and generate structures of finite amplitudes that initiate the transition process through the nonlinear interactions. The study of flow instabilities provides a better understanding of the physical mechanisms involved and can be used to build theoretical and reduced-order models for the effects associated with the structures generated during the transition process, as well as provide insight for the development of flow control strategies.

The study of the hydrodynamic instability mechanisms investigates the response of the flow to small-amplitude disturbances, which permit the linearization process of the equations Navier-Stokes. The homogeneity of the linearized equations with respect to time suggests a behavior exponential in the time for the disturbances, transforming the equations in an eigenvalue problem for modal disturbances.

In many cases of practical interest, the base flow depends solely on two of the three spatial directions. Flow quantities are then decomposed according to

$$\mathbf{q}(x,y,z,t) = \bar{\mathbf{q}}(x,y) + \varepsilon \mathbf{q}'(x,y,z,t), \tag{1}$$

where the time-independent *base flow* is prescribed as

$$\bar{\mathbf{q}} = (\bar{u}(x,y), \bar{v}(x,y), \bar{w}(x,y), \bar{T}(x,y), \bar{p}(x,y))^T. \tag{2}$$

In this case, the linear operators are homogeneous in the $z-$direction and modal disturbances take the form

$$\mathbf{q}'(x,y,z,t) \sim \hat{\mathbf{q}}(x,y)\mathrm{e}^{\mathrm{i}(\beta z - \omega t)}, \tag{3}$$

where β is a number related to a wavelength the frequency (or wavelength) $L_z = 2\pi/\beta$. The introduction of β is equivalent to performing the Fourier transform of the equations in the $z-$direction. The linear disturbance equations of two-dimensional eigenfunction problem are obtained by substituting the decomposition (1) into the governing equations, taking $\varepsilon \ll 1$, linearizing about $\bar{\mathbf{q}}$ and neglecting terms at $O(\varepsilon^2)$.

In the temporal framework, β is taken to be a real wavenumber parameter describing an eingenmode in the z-direction, while the complex ω and the eigenfunctions $\hat{\mathbf{q}}$ are sought. The real part of the eigenvalue is related with the frequency of the global eigenmode while the imaginary part is the temporal growth/damping rate. A positive value of ω_r indicates exponential growth of the instability mode in the time while ω_i indicates decay of perturbation in time. Thus, we can be written as the complex non-symmetric generalized eigenvalue problem in its most general form

$$\mathcal{L}(\bar{\mathbf{q}}, \beta, Re, Ma)\hat{\mathbf{q}} = \omega \mathcal{R}\hat{\mathbf{q}} \tag{4}$$

which these assumptions, takes the form:

$$\mathcal{L} = \begin{pmatrix} \mathcal{L}_{x,\hat{u}} & \mathcal{L}_{x,\hat{v}} & \mathcal{L}_{x,\hat{w}} & \mathcal{L}_{x,\hat{\theta}} & \mathcal{L}_{x,\hat{p}} \\ \mathcal{L}_{y,\hat{u}} & \mathcal{L}_{y,\hat{v}} & \mathcal{L}_{y,\hat{w}} & \mathcal{L}_{y,\hat{\theta}} & \mathcal{L}_{y,\hat{p}} \\ \mathcal{L}_{z,\hat{u}} & \mathcal{L}_{z,\hat{v}} & \mathcal{L}_{z,\hat{w}} & \mathcal{L}_{z,\hat{\theta}} & \mathcal{L}_{z,\hat{p}} \\ \mathcal{L}_{e,\hat{u}} & \mathcal{L}_{e,\hat{v}} & \mathcal{L}_{e,\hat{w}} & \mathcal{L}_{e,\hat{\theta}} & \mathcal{L}_{e,\hat{p}} \\ \mathcal{L}_{c,\hat{u}} & \mathcal{L}_{c,\hat{v}} & \mathcal{L}_{c,\hat{w}} & \mathcal{L}_{c,\hat{\theta}} & \mathcal{L}_{c,\hat{p}} \end{pmatrix} \tag{5}$$

$$\mathcal{R} = \begin{pmatrix} \mathcal{R}_{x,\hat{u}} & 0 & 0 & 0 & 0 \\ 0 & \mathcal{R}_{y,\hat{v}} & 0 & 0 & 0 \\ 0 & 0 & \mathcal{R}_{z,\hat{w}} & 0 & 0 \\ 0 & 0 & 0 & 0 & \mathcal{R}_{e,\hat{p}} \\ 0 & 0 & 0 & \mathcal{R}_{c,\hat{\theta}} & \mathcal{R}_{c,\hat{p}} \end{pmatrix} \tag{6}$$

This two-dimensional eigenmode problem is solved numerically using a high-order finite-difference scheme and the algorithm and numerical methods described in Gennaro *et al.* (2011); Gennaro (2012); Gennaro *et al.* (2013). After discretization, the eigenvalue problem is solved using an in-house implementation of the shift-and-invert Arnoldi algorithm.

This Krylov's subspace iteration allows for the efficient computation of an arbitrarily large window of the eigenspectrum at a small fraction of the cost of alternatives like the QZ algorithm. Matrix operators are formed and operated on in sparse format. The most demanding task in the Arnoldi algorithm, namely the LU decomposition of the matrix, is performed using the open-source library MUMPS (Amestoy *et al.*, 2001). The use of sparse storage and operations reduces drastically the computational resources required for the solution as compared to an equivalent dense-algebra computation.

3. BASE FLOW

The bubbles were generated by two-dimensional direct numerical simulation of a boundary-layer flow on a flat plate. The inflow velocity condition is a uniform flow and the bubble is generated by imposing a suction-blowing profile in the upper boundary, analogous to that produced by the pressure gradient around the nose pressure peak in medium-thickness airfoils. At the wall, a no-slip boundary condition is imposed. An isothermal wall condition is used for the temperature and the density is calculated through the compatibility condition. A zero-vorticy gradient is imposed at the far-field boundary, which together with the suction-blowing profile imposed to the wall-normal velocity produces a deceleration of the free-stream velocity.

The simulations were performed using an in-house code (Bergamo *et al.*, 2015). The code is implemented in Fortran language and parallelized with the MPI protocol using domain decomposition strategies. The compressible Navier-Stokes equations are spatially discretized using a compact finite differences scheme with spectral like resolution of 6th-order accuracy, based on Lele (1992). The temporal integration was performed by the Runge-Kuttas method of fourth order. To prevent aliasing-related problems the flow variables were filtered in the last pseudo time-step of the Runge-Kutta scheme by a 10th-order low pass filter (Visbal and Gaitonde, 2002).

In the present paper, the bubbles were obtained after a computational convergence study of mesh and domain with numeric residual of the $\sim 10^{-8}$ order. The peak reverse flow (u_{rev}/U_∞) corresponding to each combination of Reynolds and Mach numbers are presented in the Tab. 1, along with the streamwise coordinates of the separation (x_{sep}) and reattachment (x_{reat}) points.

Table 1: The values intensity levels of the reverse flow of the 2D stationary bubble.

Re	Ma=0.3	Ma=0.4	Ma=0.5	Ma=0.7
1700	9.74%	7.76%	6.45%	4.87%
2400	11.70%	9.64%	8.09%	6.22%
3100	13.70%	11.10%	9.5%	7.31%

Table 2: The separations and the reattachment points. The domain computational was $(x, y) \in [0, 100] \times [0, 3.5]$.

	x_{sep}			x_{reat}		
Re	$Ma = 0.3$	$Ma = 0.5$	$Ma = 0.7$	$Ma = 0.3$	$Ma = 0.5$	$Ma = 0.7$
1700		23.4125			32.7688	
2400	21.7198	23.0749	23.4761	34.3206	33.0036	32.1189
3100		22.8001	23.3281		33.1759	32.2342

The increase of u_{rev}/U_∞ is accompanied by a displacement of the separation and reattachment points. Therefore, for a fixed Mach number, the size of the recirculation region and the peak reversed flow grow with increasing Reynolds number. The computed separation bubbles are steady for reversed flow values up to 14%, which is in agreement with similar computations found in the literature. Figure 3shows the streamwise velocity field corresponding to the steady flow for Re = 3100 and Ma = 0.5.

4. RESULTS

The stability of the compressible laminar separation bubble flows described in section 3 is studied in the scope of the global stability analysis described in section 2. The linear stability eigenspectra was found to be dominated by a discrete eigenmode for all the combinations of Reynolds and Mach number considered.

This eigenmode shares the same characteristics of the three-dimensional instability that dominates incompressible separation bubbles (Theofilis *et al.*, 2000; Rodríguez and Theofilis, 2010; Rodríguez *et al.*, 2013). Figures 4and 4show the temporal growth rate ω_i as a function of the spanwise wavenumber β for different Reynolds numbers at Mach number 0.5 and 0.4, respectively. For each base flow with peak of reverse flow above 7%, the eigenmode is unstable for a bounded range of β, attaining its maximum amplification for a finite value, consequently corresponding to a three-dimensional perturbation.

Both the range of unstable wavenumbers and the maximum amplification is found to increase with higher Reynolds numbers, which can be due to two main reasons. On one hand, the higher the Reynolds number, the larger the recirculation region and the peak reversed flow, resulting in stronger bubbles, more prone to instability. On the other hand, for

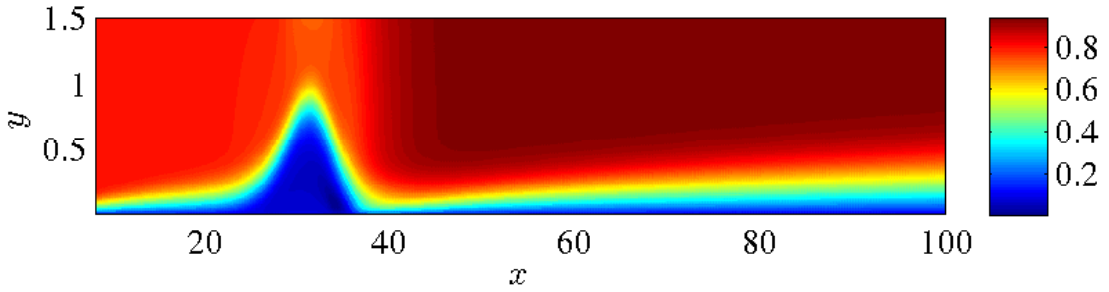

Figure 1: The velocity field of the base separation bubble corresponding to Ma=0.5 and Re=3100, with peak reversed flow $u_{rev}/U_\infty = 9.5\%$.

centrifugal instabilities like the present one, viscosity has a stabilizing effect which is reduced with increasing values of the Reynolds number.

The influence of Mach number maintaining fixed the Reynolds Number on this mode shows that the compressibility has a stabilizing effect, as can be seen in Fig. 4. However, for reverse flow peak level fixed around around 9%, the Mach number has a different behavior, as can be seen in Fig. 4.

The eigenfunctions, illustrating the spatial structure of the modal perturbation, are highly localized in the vicinity of the recirculation region, as shown in fig. 4.

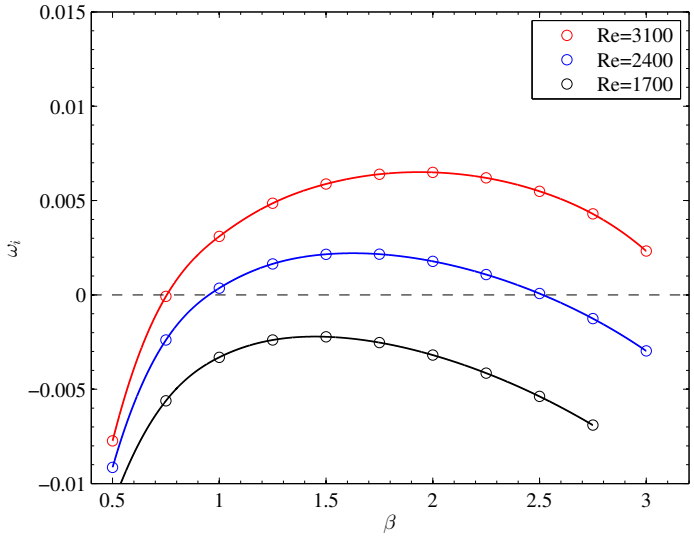

Figure 2: Temporal amplification rate ω_i against spanwise wavenumber β for the steady three-dimensional global mode at $Ma = 0.5$.

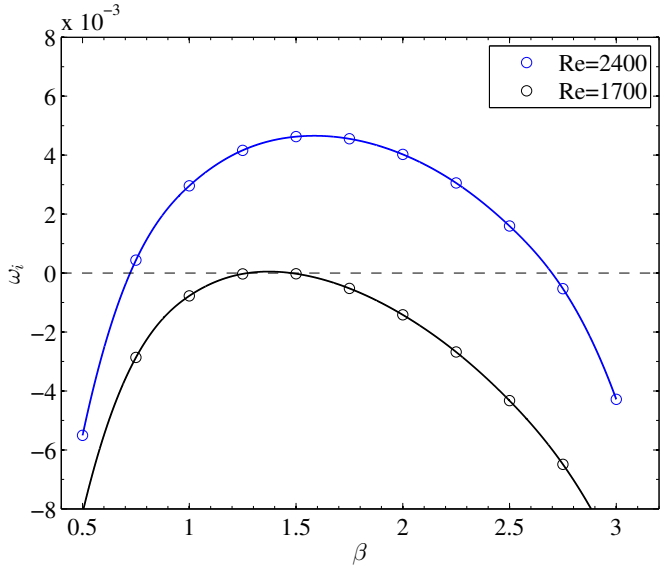

Figure 3: Temporal amplification rate ω_i against spanwise wavenumber β for the steady three-dimensional global mode at $Ma = 0.4$.

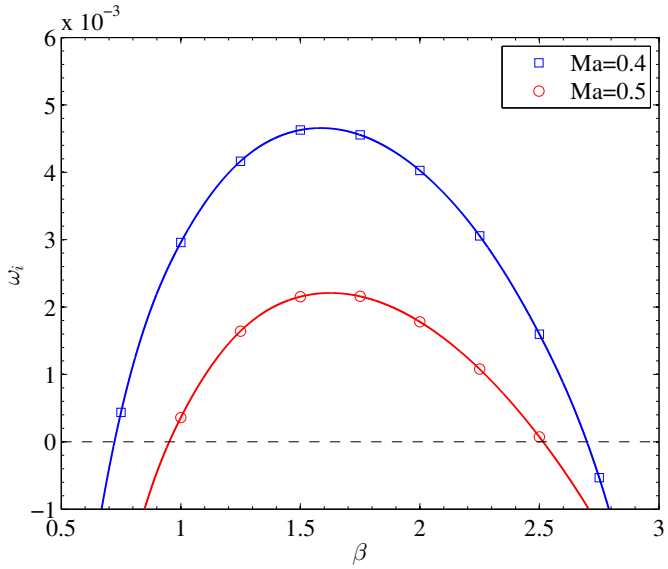

Figure 4: Temporal amplification rate ω_i against spanwise wavenumber β for the steady three-dimensional global mode at $Re = 2400$ for $Ma = 0.5$ and $Ma = 0.4$.

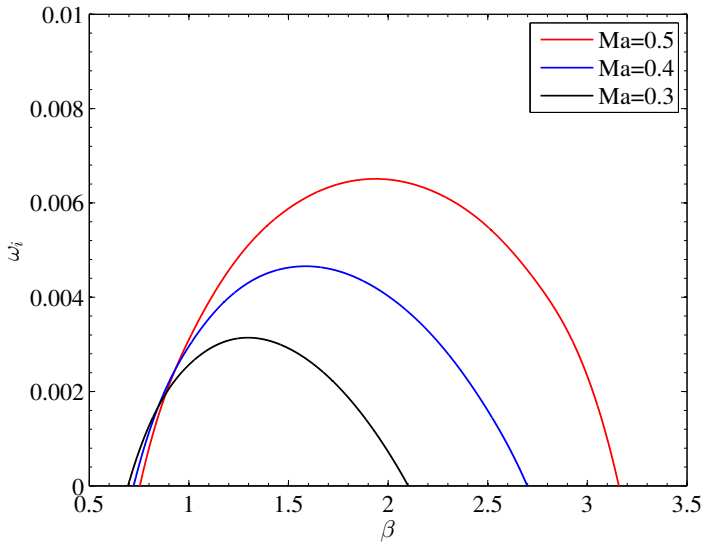

Figure 5: Temporal amplification rate ω_i against spanwise wavenumber β for a peak reversed of 9%.

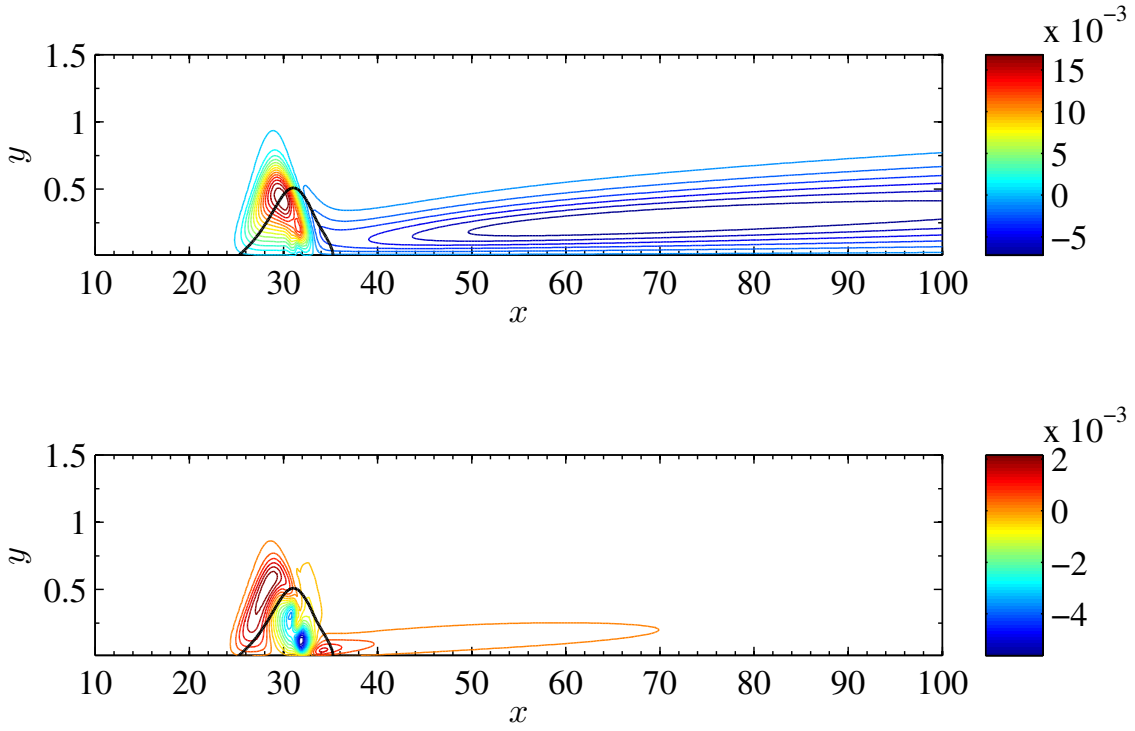

Figure 6: Streamwise velocity component of the most unstable eigenmode for the base separation bubble corresponding to $Ma = 0.5, Re = 3100$ ($\beta = 2.5$ and $\omega_i = 0.005504$).

5. CONCLUSIONS

The combined influence of the Reynolds and Mach numbers on the linear instability of laminar separation bubbles in the absent of environmental or externally introduced disturbances is studied here, thus extending the work done in Rodríguez *et al.* (2013) to compressible flow. A validated direct numerical simulation code is used to compute a family of model separation bubbles on a flat-plate boundary layer with different Reynolds and Mach numbers. Steady two-dimensional flows with peak reversed up to 16% were computed in this manner, thus bounding the parametric region for the onset of periodic vortex shedding. A modal stability analysis was performed for these steady flows, which showed the dominance of a discrete three-dimensional eigenmode analogous to the one found for incompressible bubbles in previous researches. Reynolds number has a clear destabilizing effect, partly due to the modifications on the base flow, partly due to the reduced viscous damping of the centrifugal instability. The role of the Mach number is more involved, and requires of further investigations in order to isolate its effect on the base flow (measured through the peak reversed flow) and on the centrifugal instability eigenmode.

6. ACKNOWLEDGMENTS

This work is supported by São Paulo Research Foundation (FAPESP) grants 2014/24782-0. The work of D.R. is funded by the Science without borders/CAPES- "Attraction of Young Talents" Fellowship. The work of B.D.P.S. is funded by São Paulo Research Foundation (FAPESP) 2015/26759-9.

7. REFERENCES

Amestoy, P.R., Duff, I.S., L'Excellent, J.Y. and Koster, J., 2001. "A fully asynchronous multifrontal solver using distributed dynamic scheduling". *SIAM J. Matrix Anal. Appl.*, Vol. 23, No. 1, pp. 15–41. ISSN 0895-4798.

Bergamo, L., Gennaro, E.M., Theofilis, V. and Medeiros, M., 2015. "Compressible modes in a square lid-driven cavity". *Aerospace Science and Technology*, Vol. 44, pp. 125 – 134.

Dallmann, U., 1988. "Three-dimensional vortex structures and vorticity topology". *Fluid Dynamics Resarch*, , No. 3, pp. 183–189.

Diwan, S. and Ramesh, O., 2012. "Relevance of local parallel theory to the linear stability of laminar separation bubbles". *J. Fluid Mech.*, Vol. 698, pp. 468–478.

Embacher, M. and Fasel, H.F., 2014. "Direct numerical simulations of laminar separation bubbles: investigation of absolute instability and active flow control of transition to turbulence". *Journal of Fluid Mechanics*, Vol. 747, pp. 141–185.

Gennaro, E.M., 2012. *Análise da estabilidade global de escoamentos compressíveis*. Ph.D. thesis, Universidade de São Paulo.

Gennaro, E.M., Rodríguez, D. and Souza, L.F., 2015. "Secondary instability analysis of 3d laminar separation bubbles based on cross-plane wkb approximation". In *Proceedings of 23rd ABCM International Congress of Mechanical Engineering*.

Gennaro, E.M., Rodríguez, D., Theofilis, V. and Medeiros, M.A.F., 2013. "Sparse techniques in global flow instability with application to compressible leading-edge flow". *AIAA Journal*, Vol. 51, No. 9, pp. 2295 – 2303.

Gennaro, E.M., Rodríguez, D.A., Theofilis, V. and Medeiros, M.A.F., 2011. "Linear instability of orthogonal compressible leading-edge boundary layer flow". *AIAA-paper*, , No. 2011-3751.

Lele, S., 1992. "Compact finite difference schemes with spectral-like resolution". *Journal of Computational Physics*, Vol. 103, No. 1, pp. 16–42.

Lin, C.C., 1955. *The Theory of Hydrodynamic stability*. Cambridge University Press.

Marxen, O., Lang, M. and Rist, U., 2013. "Vortex formation and vortex breakup in laminar separation bubbles". *J. Fluid Mech.*, Vol. 728, pp. 58–90.

Rist, U. and Maucher, U., 1994. "Direct numerical simulation of 2–d and 3–d instability waves in a laminar separation bubble". In B. Cantwell, ed., *AGARD-CP-551 Application of Direct and Large Eddy Simulation to Transition and Turbulence*. pp. 34–1 – 34–7.

Rist, U. and Maucher, U., 2002. "Investigations of time-growing instabilities in laminar separation bubbles". *European Journal of Mechanics - B/Fluids*, Vol. 21, No. 5, pp. 495 – 509. ISSN 0997-7546.

Rodríguez, D. and Gennaro, E.M., 2015. "On the secondary instability of forced and unforced laminar separation bubbles". *Procedia IUTAM*, Vol. 14, pp. 78 – 87.

Rodríguez, D., Gennaro, E.M. and Juniper, M.P., 2013. "The two classes of primary modal instability in laminar separation bubbles". *J. Fluid Mech.*, Vol. 734, p. R4.

Rodríguez, D. and Theofilis, V., 2010. "Structural changes of laminar separation bubbles induced by global linear instability". *J. Fluid Mech.*, Vol. 655, pp. 280 – 305.

Theofilis, V., Hein, S. and Dallmann, U., 2000. "On the origins of unsteadiness and three-dimensionality in a laminar separation bubble". *Phil. Trans. R. Soc. Lond.*, Vol. 358, No. 1777, pp. 3229 – 3246.

Visbal, M.R. and Gaitonde, D.V., 2002. "On the Use of Higher-Order Finite-Difference Schemes on Curvilinear and Deforming Meshes". *Journal of Computational Physics*, Vol. 181, No. 1, pp. 155–185.

8. RESPONSIBILITY NOTICE

The authors are the only responsible for the printed material included in this paper.